Acta Crystallographica Section D
Biological Crystallography
ISSN 0907-4449

Structure of xylose isomerase from *Streptomyces diastaticus* No. 7 strain M1033 at 1.85 Å resolution

Xue-yong Zhu,[a,b] Mai-kun Teng,[a,b] Li-wen Niu,[a,b,c]* Chong Xu[a] and Yu-zhen Wang[a]

[a]Department of Molecular and Cell Biology, School of Life Sciences, University of Science and Technology of China, 96 Jinzhai Road, Hefei, Anhui 230026, People's Republic of China, [b]Laboratory of Structural Biology, School of Life Sciences, University of Science and Technology of China, 96 Jinzhai Road, Hefei, Anhui 230026, People's Republic of China, and [c]National Laboratory of Biomacromolecules, Institute of Biophysics, Chinese Academy of Science, 15 Datun Road, Beijing 100101, People's Republic of China

Correspondence e-mail: lwniu@ustc.edu.cn

Received 14 April 1999
Accepted 18 November 1999

PDB Reference: SDXyI, 1qt1.

The structure of xylose isomerase (XyI) from *Streptomyces diastaticus* No. 7 strain M1033 (SDXyI) has been refined at 1.85 Å resolution to conventional and free *R* factors of 0.166 and 0.219, respectively. SDXyI was crystallized in space group $P2_12_12$, with unit-cell parameters a = 87.976, b = 98.836, c = 93.927 Å. One dimer of the tetrametric molecule is found in each asymmetric unit. Each monomer consists of two domains: a large N-terminal domain (residues 1–320), containing a parallel eight-stranded α/β barrel, and a small C-terminal loop (residues 321–387), containing five helices linked by random coil. The four monomers are essentially identical in the tetramer, possessing non-crystallographic 222 symmetry with one twofold axis essentially coincident with the crystallographic twofold axis in the space group $P2_12_12$, which may explain why the diffraction pattern has strong pseudo-$I222$ symmetry even at medium resolution. The crystal structures of XyIs from different bacterial strains, especially from *Streptomyces*, are similar. The $\alpha2$ helix of the α/β barrel has a different position in the structures of different XyIs. The conformation of C-terminal fragment 357–364 in the SDXyI structure has a small number of differences to that of other XyIs. Two Co^{2+} ions rather than Mg^{2+} ions exist in the active site of the SDXyI structure; SDXyI seems to prefer to bind Co^{2+} ions rather than Mg^{2+} ions.

1. Introduction

Xylose isomerase (XyI; E.C. 5.3.1.5) has been extensively studied in several laboratories. The enzyme was widely found in a number of bacteria and catalyzes the isomerization of D-xylose to D-xylulose *in vivo*. The practical significance of the enzyme stems from its ability to isomerize D-glucose to D-fructose under certain conditions *in vitro*; therefore, the enzyme is often referred to as glucose isomerase and utilized in industry for the production of high-fructose corn syrup.

In addition to its commercial importance, XyI is interesting as a protein model for the study of the structure–function relationships of biomacromolecules, particularly for kinetic studies, since the reaction catalyzed by the enzyme is a single-substrate/single-product interconversion and the turnover rate for the substrate is relatively low.

Moreover, XyI is a metal-ion dependent enzyme. Mg^{2+}, Co^{2+} and Mn^{2+} ions activate the enzyme, whereas Ni^{2+}, Ca^{2+}, Ba^{2+}, Zn^{2+}, Cu^{2+} and Hg^{2+} ions do not (Callens *et al.*, 1986; Danno, 1970). The stability of the enzyme also depends on the number and type of divalent metal ions presented. It was shown that addition of one Co^{2+} ion could enhance the structural stability of *S. violaceoruber* XyI and that a second Co^{2+} ion was required for its activity (Callens *et al.*, 1988). The Co^{2+} ion was better than the Mg^{2+} ion in protecting the

enzyme against thermal denaturation (Danno, 1971; Callens *et al.*, 1988). It was also found that Co^{2+} and Mn^{2+} ions bind to the two sites with a higher affinity than Mg^{2+} ions (van Tilbeurgh *et al.*, 1992).

In order to understand and explain the reaction mechanism, the crystal structures of XyIs, including native enzymes, complexes bound with different substrates, inhibitors or metal ions and mutants with specific amino-acid residues selected, have been solved from different bacterial strains, such as *Actinoplanes missouriensis* (AM; Rey *et al.*, 1988; Jenkins *et al.*, 1992; Lambeir *et al.*, 1992; van Tilbeurgh *et al.*, 1992), *Arthrobacter* strain B3728 (AB; Henrick *et al.*, 1989; Collyer *et al.*, 1990), *S. olivochromogenes* (SO; Farber *et al.*, 1987; Lavie *et al.*, 1994; Allen *et al.*, 1995), *S. rubiginosus* (SR; Carrell *et al.*, 1984, 1989, 1994; Whitlow *et al.*, 1991), *S. albus* (SA; Dauter *et al.*, 1990), *S. murinus* (SM; Rasmussen *et al.*, 1994) and *S. diastaticus* No. 7 strain M1033 (SD; Zhu *et al.*, 1996). A possible reaction mechanism involving a hydride shift has been proposed (Farber *et al.*, 1987; Collyer *et al.*, 1990; Whitlow *et al.*, 1991; Jenkins *et al.*, 1992; van Tilbeurgh *et al.*, 1992; Carrell *et al.*, 1994). Another mechanism involving an enediol intermediate has also been suggested, similar to that of triose phosphate isomerase (Rose *et al.*, 1969).

The XyIs have been reported to be either tetramers or dimers in solution, depending on the source. However, no matter what space group the crystals belong to, the XyIs all exist in a tetrameric form in the crystal structures reported; the monomers in the tetramer are related to each other strictly or approximately by the point group 222. Each monomer consists of an N-terminal major domain folded as an eight-stranded α/β barrel and a C-terminal minor domain folded as a large loop. There are three types of XyI aggregation in the asymmetric units: monomer (*e.g.* SRXyI and SAXyI), dimer (*e.g.* ABXyI, SOXyI and SMXyI) or tetramer (*e.g.* AMXyI).

The monomer of XyI from *S. diastaticus* No. 7 strain M1033 (SDXyI) consists of 387 amino-acid residues, has a molecular weight of 43 kDa and shows a high sequence homology with the XyIs from other *Streptomyces* species mentioned above (>90%; Wang *et al.*, 1994). The crystals of SDXyI possess a strong pseudo-*I*222 symmetry, similar to that of SOXyI (Farber *et al.*, 1987; Lavie *et al.*, 1994). The body centring is obeyed very well at lower resolution, but the diffraction intensities of the body-centred reflections become significant at higher diffraction angles. The correct crystallographic space group should be primitive and one of the sub-groups of *I*222, with a dimer in the asymmetric unit. However, the correct space group could not be confirmed directly from the diffraction data in our previous paper (Zhu *et al.*, 1996), in which the pseudo-*I*222 SDXyI structure was determined at 1.9 Å resolution in order to supply targets as rapidly as possible for the related site-directed mutagenesis. In other words, the SDXyI structure reported is an averaged structure of the two monomer molecules in the asymmetric unit. Here, we report the crystal structure of the enzyme at higher resolution (1.85 Å) in the correct crystallographic space group, reconfirm the type of metal ions in the active site and the structural details, and provide some comparisons between the structures of SDXyI and other XyIs in order to indicate the structural features of XyI.

Table 1
Statistics of data collection and structural refinement of SDXyI.

Space group	$P2_12_12$
Unit-cell parameters (Å)	
a	87.976
b	98.836
c	93.297
Resolution range (Å)	5.0–1.85
Independent reflections	55237
Completeness (%)	82.8
Last-shell completeness (%)†	72.8
R_{merge}‡	8.0
Number of water molecules	636
Number of metal ions	4
R_{cryst}§	0.166
R_{free}§	0.219
Bond-length r.m.s. deviation (Å)	0.011
Bond-angle r.m.s. deviation (°)	1.567
Average temperature factors (Å^2)	
All atoms	12.54
Protein atoms	10.70
Main-chain atoms	8.98
Side-chain atoms	12.53
Water molecules	29.96

† The last shell is from 1.93 to 1.85 Å. ‡ $R_{merge} = \sum|I - \langle I\rangle|/\sum|I|$, where I is the observed diffraction intensity and $\langle I\rangle$ is the average diffraction intensity from several measurements for one reflection. The summation is over all reflections. § $R = \sum||F_o| - |F_c||/\sum|F_o|$, where F_o and F_c are the observed and calculated structure factors, respectively. The conventional crystallographic R factor (R_{cryst}) and free R factor (R_{free}) are calculated using the work and test reflection sets, respectively.

2. Materials and methods

SDXyI was purified and crystallized as reported previously (Zhang *et al.*, 1991). The crystals were grown at room temperature (~293 K) by the sitting-drop vapour-diffusion technique from 10 mg ml^{-1} protein solution in 0.02 *M* Tris–HCl buffer pH 7.5, 1.0 *M* $(NH_4)_2SO_4$, 0.01 *M* $MgCl_2$, 0.001 *M* $CoCl_2$ equilibrated against 0.02 *M* Tris–HCl buffer pH 7.5, 2.0 *M* $(NH_4)_2SO_4$. X-ray diffraction data were collected at room temperature on a Siemens X200B multiwire area detector mounted on a Rikagu rotating-anode X-ray generator using a copper anode (50 kV, 200 mA) at the National Laboratory of Biomacromolecules, Beijing. The crystals were very stable in the X-ray beam, allowing the collection of an extensively replicated data set to 1.85 Å from a single crystal (the redundancy of the data was about 4.0). The *XENGEN* software package (Howard *et al.*, 1987) was used for data reduction in space group *P*222. The data-collection and reduction statistics are shown in Table 1.

According to the analysis of the crystallographic symmetry, the correct space group of the SDXyI crystals should be one of the four sub-groups of *I*222: $P2_122_1$, $P2_12_12$, $P22_12_1$ and *P*222 (unit-cell parameters $a = 87.976$, $b = 98.836$, $c = 93.927$ Å), with a dimer in the asymmetric unit. The averaged structure of the enzyme monomers refined in pseudo-*I*222 was used as the starting model, with the deletion of metal ions and water molecules and the assignment of temperature factors of 15.0 Å^2 to all atoms. The initial positions of four possible

dimers in the asymmetric unit were generated from this model by applying the transformation matrices between the pseudo-space group $I222$ and the space groups $P2_122_1$, $P2_12_12$, $P22_12_1$ and $P222$. Using the data with $F_{obs} > 2.0\sigma(F_{obs})$ to 1.85 Å resolution, all four dimers produced were subjected to refinement by *X-PLOR* (Brünger, 1992*a*). A test data set containing 10% of the reflections was selected and reserved for the calculation and examination of a free R factor (R_{free}; Brünger, 1992*b*) throughout the refinement process. Loose non-crystallographic symmetry (NCS) restraints were utilized in the refinement of the atomic positions and temperature factors; the atomic positions of side chains were restrained more loosely than those of the main chain. With one cycle of rigid refinement and two cycles of conventional restrained positional refinement and individual temperature-factor refinement, the dimers generated in space groups $P2_12_12$, $P22_12_1$, $P2_1221$ and $P222$ gave R factors (R_{cryst}) and R_{free} values of 0.216 and 0.263, 0.308 and 0.369, 0.316 and 0.393, and 0.316 and 0.383, respectively; the dimer generated in space group $P2_12_12$ gave the lowest R_{cryst} and R_{free}, which were almost 0.1 lower than those generated in the other three space groups; the space group $P2_12_12$ was therefore selected as the correct one.

With the program packages *O* (Jones *et al.*, 1991) and *CHAIN* (Sack, 1988), the initial $2F_o - F_c$ and $F_o - F_c$ maps generated to 1.85 Å using *X-PLOR* (Brünger, 1992*a*) showed that the model fitted the electron density well except for parts of the side chains, which were rebuilt by hand. 525 water molecules were added using the *X-PLOR* 3.851 program *WATERPICK* and were checked individually for their fit to the $2F_o - F_c$ and $F_o - F_c$ maps at 1.8σ cutoff. The $2F_o - F_c$ map showed that two relatively strong electron-density peaks representing the intrinsic metal ions were clear in each monomer at positions similar to those in the structures of other xylose isomerases. Considering that Mg^{2+} and Co^{2+} ions were both used in the crystallization and that the concentration of Mg^{2+} was ten times higher than that of Co^{2+}, the Mg^{2+} ions were added as a first trial; in each monomer, one Mg^{2+} was tetracoordinated and another Mg^{2+} was hexacoordinated. Further positional and temperature-factor refinements were performed, resulting in an R_{cryst} and R_{free} of 0.220 and 0.180, respectively. However, the $F_o - F_c$ map at this point still showed strong residual electron-density peaks at the positions of all four Mg^{2+} ions in the dimer and the temperature factors of all four Mg^{2+} ions dropped to 2.0 Å^2; the Mg^{2+} ions were therefore all replaced by Co^{2+} ions in the subsequent refinement process. Three shells of further water molecules were then added and examined. NCS restraints were not utilized in the last two refinement cycles. The changes in the R_{free} value were monitored throughout the refinement.

```
                10        20        30        40        50        60
SD SYQPTPEDKFTFGLWTVGWQGRDPFGDATRGALDPAESVRRLAELGAHGVTFHDDDLIPF
SR NYQPTPEDRFTFGLWTVGWQGRDPFGDATRRALDPVESVRRLAELGAHGVTFHDDDLIPF
SO SYQPTPEDRFTFGLWTVGWQGRDPFGDATRPALDPVETVQRLAELGAHGVTFHDDDLIPF
SA NYQPTPEDRFTFGLWTVGWEGRDPFGDATRTALDPVESVRRLAELGAHGVTFHDDDLIPF
SM SFQPTPEDRFTFGLWTVGWQGRDPFGDATRPALDPVETVQRLAELGAYGVTFHDDDLIPF
AB SVQPTPADHFTFGLWTVGWTGADPFGVATRKNLDPVEAVHKLAELGAYGITFHDNDLIPF
AM SVQATREDKFSFGLWTVGWQARDAFGDATRTALDPVEAVHKLAEIGAYGITFHDDDLVPF

            70        80        90        100       110       120
SD GATDSERAEHIKRFRQALDETGMKVPMATTNLFTHPVFKDGGFTANDRDVRRYALRKTIR
SR GSSDSEREEHVKRFRQALDDTGMKVPMATTNLFTHPVFKDGGFTANDRDVRRYALRKTIR
SO GSSDTERESHIKRFRQALDATGMTVPMATTNLFTHPVFKDGGFTANDRDVRRYALRKTIR
SA GSSDSERYEHVKRFRQALDDTGMKVPMATTNLFTHPVFKDGGFTANDRDVRRYALRKTIR
SM GSSDTERESHIKRFRQALDATGMTVPMATTNLFTHPVFKDGGFTANDRDVRRYALRKTIG
AB DATEAEREKILGDFNQALKDTGLKVPMVTTNLFSHPVFKDGGFTSNDRSIRRFALAKVLH
AM GSDAQTRDGIIAGFKKALDETGLIVPMVTTNLFTHPVFKDGGFTSNDRSVRRYAIRKVLR

            130       140       150       160       170       180
SD NIDLAVELGAQTYVAWGGREGAESGAAKDVRVALDRMKEAFDLLGEYVTSQGYDTAFAIE
SR NIDLAVELGAETYVAWGGREGAESGGAKDVRDALDRMKEAFDLLGEYVTSQGYDIRFAIE
SO NIDLAVELGAKTYVAWGGREGAESGAAKDVRVALDRMKEAFDLLGEYVTSQGYDTRFAIE
SA NIDLAVELGAETYVAWGGREGAESGGAKDVRDALDRMKEAFDLLGEYVTSQGYDIRFAIE
SM NIDLAAELGAKTYVAWGGREGAESGGAKDVRDALDRMKEAFDLLGEYVTAQGYDLRFAIE
AB NIDLAAEMGAETFVMWGGREGSEYDGSKDLAAALDRMREGVDTAAGYIKDKGYNLRIALE
AM QMDLGAELGAKTLVLWGGREGAEYDSAKDVSAALDRYREALNLLAQYSEDRGYGLRFAIE

            190       200       210       220       230       240
SD PKPNEPRGDILLPTIGHALAFIDGLERPELYGVNPEVGHEQMAGLNFPHGIAQALWAGKL
SR PKPNEPRGDILLPTVGHALAFIERLERPELYGVNPEVGHEQMAGLNFPHGIAQALWAGKL
SO PKPNEPRGDILLPTVGHALAFIERLERPELYGVNPEVGHEQMAGLNFPHGIAQALWAGKL
SA PKPNEPRGDILLPTVGHALAFIERLERPELYGVNPEVGHEQMAGLNFPHGIAQALWAGKL
SM PKPNEPRGDILLPTVGHALAFIERLERPELYGVNPEVGHEQMAGLNFPHGIAQALWAGKL
AB PKPNEPRGDIFLPTVGHGLAFIEQLEHGDIVGLNPETGHEQMAGLNFTHGIAQALWAEKL
AM PKPNEPRGDILLPTAGHAIAFVQELERPELFGINPETGHEQMSNLNFTQGIAQALWHKKL

            250       260       270             280       290
SD FHIDLNGQSGIKYDQDLRFGAGDLRAAFWLVDLLESA------GYEGPRHFDFKPPRTED
SR FHIDLNGQNGIKYDQDLRFGAGDLRAAFWLVDLLESA------GYSGPRHFDFKPPRTED
SO FHIDLNGQSGIKYDQDLRFGAGDLRAAFWLVDLLESA------GYEGPRHFDFKPPRTED
SA FHIDLNGQNGIKYDQDLRFGAGDLRAAFWLVDLLESA------GYSGPRHFDFKPPRTED
SM FHIDLNGQSGIKYDQDLRFGAGDLRAAFWLVDLLETA------GYEGPRHFDFKPPRTED
AB FHIDLNGQRGIKYDQDLVFGHGDLTSAFFTVDLLENGFPNGGPKYTGPRHFDYKPSRTDG
AM FHIDLNGQHGPKFDQDLVFGHGDLLNAFSLVDLLENG-PDGAPAYDGPRHFDYKPSRTED

          300       310       320       330       340       350
SD FDGVWASAAGCMRNYLILKERAAAFRADPEVQEALRAARLDELAQPTAGDGLQA--LLAD
SR FDGVWASAAGCMRNYLILKERAAAFRADPEVQEALRASRLDELARPTAADGLQA--LLDD
SO IDGVWASAAGCMRNYLILKERAAAFRADPEVQEALRASRLDELAQPTAADGVQE--LLAD
SA FDGVWASAAGCMRNYLILKERAAAFRADPEVQEALRASRLDELARPTAADGLQA--LLDD
SM FDGVWASAAGCMRNYLILKDRAAAFRADPEVQEALRAARLDQLAQPTAADGLDA--LLAD
AB YDGVWDSAKANMSMYLLLKERALAFRADPEVQEAMKTSGVFELGETTLNAGESAADLMND
AM YDGVWESAKANIRMYLLLKERAKAFRADPEVQEALAASKVAELKTPTLNPGEGYAELLAD

          360       370       380
SD RSAFEDFDPDAAAARGMAFERLDQLAMDHLLGARG
SR RSAFEEFDVDAAAARGMAFERLDQLAMDHLLGARG
SO RTAFEDFDVDAAAARGMAFERLDQLAMDHLLGAR
SA RSAFEEFDVDAAAARGMAFERLDQLAMDHLLGARGAAA
SM RAAFEDFDVDAAAARGMAFEHLDQLAMDHLLGARG
AB SASFAGFDAEAAAERNFAFIRLNQLAIEHLLGSR
AM RSAFEDYDADAVGAKGFGFVKLNQLAIEHLLGAR
```

Figure 1
The sequences of seven xylose isomerases for which crystal structures have been reported. SD, *S. diastaticus* No. 7 strain M1033 (Wang *et al.*, 1994); SR, *S. rubiginosus* (Wong *et al.*, 1991); SO, *S. olivochromogenes* (Lavie *et al.*, 1994); SA, *S. albus* (Dauter *et al.*, 1990); SM, *S. murinus* (Rasmussen *et al.*, 1994); AB, *Arthrobacter* strain B3728 (Loviny-Anderton *et al.*, 1991); AM, *Actinoplanes missouriensis* (Amore & Hollenberg, 1989).

3. Results and discussion

3.1. The structural refinement and overall structure

6020 protein atoms, 636 water molecules and four Co^{2+} ions were included in the final structural model of SDXyI in space

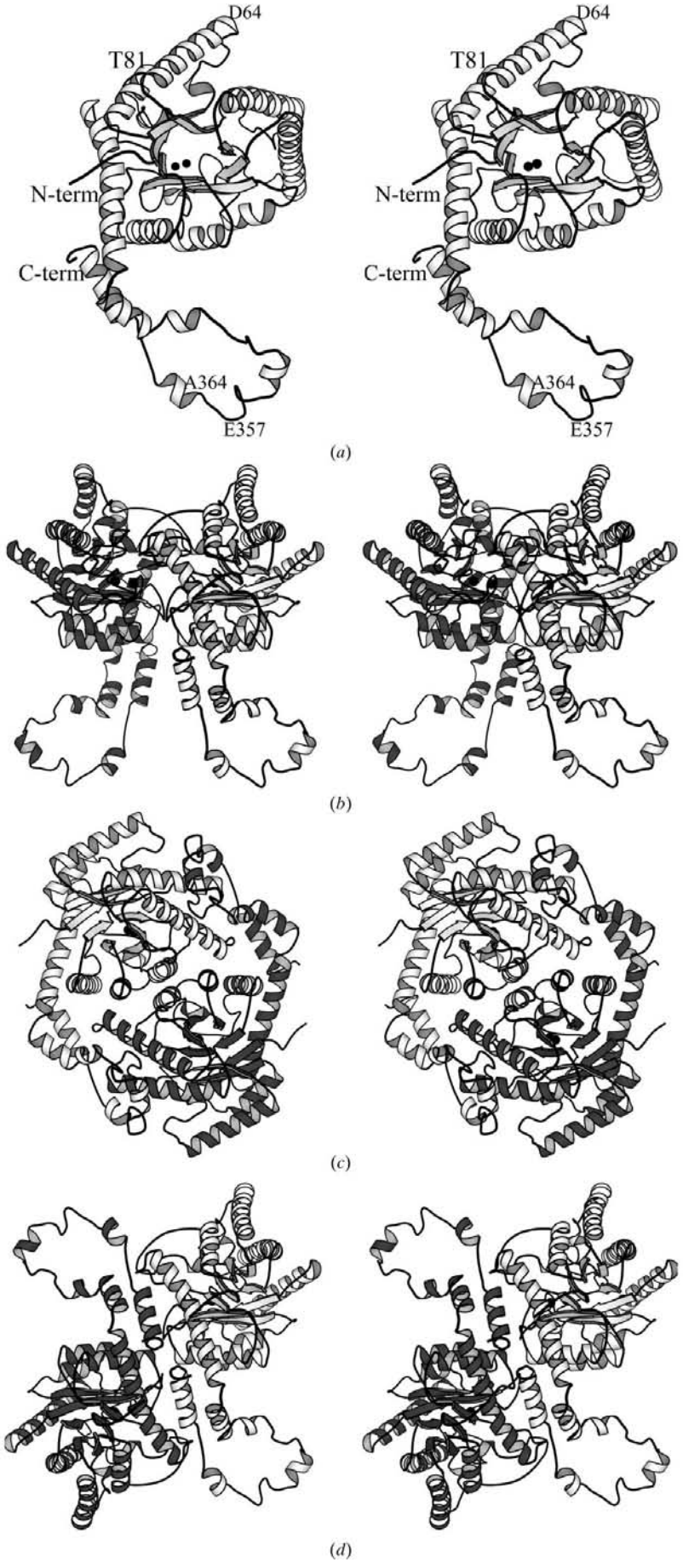

group $P2_12_12$, with unit-cell parameters a = 87.976, b = 98.836, c = 93.927 Å and a dimer in the asymmetric unit, leading to final R_{cryst} and R_{free} values of 0.166 and 0.219, respectively, for diffraction data to 1.85 Å resolution (Table 1). The accuracy of the atomic positions in the refined model was estimated to be about 0.20 Å on the basis of the dependence of the R_{cryst} values on resolution (Luzzati, 1952).

All main-chain atoms had satisfactory electron density in the final $2F_o - F_c$ maps. There were no uninterpretable features on the maps significantly higher than the noise level. However, a few long side chains, especially the charged side chains of lysine residues on the molecular surface, were poorly resolved owing to the poor electron density.

Most of the residues have main-chain dihedral angles that lie within or very near the acceptable regions of a Ramanchandran plot (data not shown). Of particular note is Glu185, adjacent to Pro186 which adopts a *cis* conformation.

The average temperature factor for all atoms is 12.54 Å^2. Generally, there is a close correspondence between the temperature factors of equivalent residues in the two subunits. For the well ordered residues within the active sites of the two subunits, the average temperature factors are 6.77 and 6.56 Å^2, respectively. The temperature factors of the two Co^{2+} ions in sites 1 and 2 of subunit *A* are 16.14 and 10.22 Å^2, respectively; the temperature factors are 18.03 and 11.02 Å^2 in sites 1 and 2, respectively, of subunit *B*.

The overall structure of each monomer consists of two domains: a large N-terminal domain (residues 1–320), containing a parallel eight-stranded α/β barrel, and a small C-terminal loop (residues 321–387), containing five helices linked by random coil (Fig. 2*a*). There is a dimer in the asymmetric unit; two dimers form a tetramer possessing the non-crystallographic 222 symmetry, with one twofold axis essentially coincident with the crystallographic twofold axis in space group $P2_12_12$ (Fig. 2*b*). The model of each monomer in the asymmetric unit was rebuilt independently during refinement. The r.m.s.

Figure 2
The C^{α} tracings of the SDXyI structure: (*a*) monomer, the α2 helix Asp64–Thr81 of the α/β-barrel; the fragment Glu357–Ala364 and the metal sites are indicated, (*b*) 'butterfly' dimer or asymmetric unit dimer, (*c*) 'yin–yang' dimer and (*d*) 'diagonal' dimer. The figures were rendered using *MOLSCRIPT* (Kraulis, 1991).

Table 2
The r.m.s. deviations (Å) of C^{α} coordinates from positions 3–386 and (in parentheses) 3–320 of the seven XyI structures.

	SRXyI	SAXyI	SOXyI	SMXyI	ABXyI	AMXyI
SDXyI	0.264 (0.228)	0.273 (0.243)	0.245 (0.198)	0.950 (0.407)	0.882 (0.772)	0.857 (0.667)
SRXyI		0.091 (0.095)	0.256 (0.230)	0.939 (0.379)	0.902 (0.770)	0.857 (0.667)
SAXyI			0.251 (0.228)	0.937 (0.374)	0.904 (0.772)	0.860 (0.673)
SOXyI				0.944 (0.396)	0.912 (0.785)	0.825 (0.651)
SMXyI					1.197 (0.859)	1.269 (0.725)
ABXyI						1.135 (0.923)

Table 3
The r.m.s. deviations (Å) of C^{α} coordinates from positions 64–81 of seven XyI structures.

Data shown are the r.m.s. deviations (Å) calculated after applying the best superimpositions of C^{α} positions 64–81. Data in parentheses are the r.m.s. deviations calculated after applying the best superimpositions of C^{α} positions 3–63 together with 82–320.

	SRXyI	SAXyI	SOXyI	SMXyI	ABXyI	AMXyI
SDXyI	0.256 (0.668)	0.243 (0.677)	0.220 (0.438)	0.433 (0.758)	0.313 (0.753)	0.360 (0.709)
SRXyI		0.098 (0.11)	0.230 (0.521)	0.340 (0.464)	0.201 (0.893)	0.220 (0.547)
SAXyI			0.205 (0.499)	0.323 (0.424)	0.230 (0.943)	0.235 (0.563)
SOXyI				0.407 (0.521)	0.251 (0.942)	0.321 (0.581)
SMXyI					0.328 (1.11)	0.360 (0.639)
ABXyI						0.261 (0.793)

deviations of all atoms and C^{α} atoms between the two monomers are 0.145 and 0.072 Å, respectively, which are comparable with the error level estimated on the basis of the crystallographic *R* factor. This experimental fact implies that the four monomers in the tetramer are essentially identical and may explain why the diffraction pattern has strong pseudo-*I*222 symmetry even at medium resolution. The initial 1.90 Å resolution structure (Zhu *et al.*, 1996) was solved in the pseudo-*I*222 space group and only one monomer was found in the symmetric unit. Comparing the subunits *A* and *B* with the initial model, the r.m.s. deviations between the main-chain atoms are all 0.19 Å and the r.m.s deviations between the side-chain atoms are 0.90 and 0.89 Å, respectively; in other words, the main differences between the initial and refined models are focused on the side-chain atoms.

3.2. Comparison of the SDXyI structure with other XyIs

In order to investigate the structure features of all xylose isomerases, the native structures of ABXyI (Protein Data Bank entry 1xlk; Collyer *et al.*, 1990), AMXyI (4xim; Jenkins *et al.*, 1992), SRXyI (7xia; Carrell *et al.*, 1989), SOXyI (1xya; Lavie *et al.*, 1994), SAXyI (6xia; Dauter *et al.*, 1990), SMXyI (1dxi; Rasmussen *et al.*, 1994) and the refined structure of SDXyI in this paper were chosen for comparison. Only subunit *A* was used for superimposition if the asymmetric unit had more than one subunit. The transformation for the superimposition of the coordinates was determined by the algorithm of Hendrickson & Konnert (1981).

Among these seven XyIs, the enzymes from *Streptomyces* species show large sequence homologies of up to >90% and have about 70% sequence identity with ABXyI or AMXyI (the sequences of the seven XyIs are shown in Fig. 1). Comparison of the backbone structures of SRXyI and ABXyI (Henrick *et al.*, 1987) showed an insertion of six amino acids at position 277 and two individual insertions at positions 348 and 357 (numbering according to the SRXyI structure). The amino-acid residues inserted were omitted in the course of our comparisons. All seven structures were superimposed on each other. The r.m.s. deviations of C^{α} coordinates from positions 3–386 (hereafter, numbering is according to the SDXyI structure except where noted) are listed in Table 2, which shows a high degree of structural homology between the seven molecules. The structures of the XyIs from *Streptomyces* species are very similar except for SMXyI, which has some significant displacements. A more precise superimposition can be obtained using the C^{α} positions 3–320 excluding the C-terminal loop (data also shown in Table 2).

The r.m.s. deviations between SDXyI and other *Streptomyces* XyIs are small except for SMXyI (data not shown). Relatively large displacements occur in several residue fragments between SDXyI and ABXyI or AMXyI (data not shown), which might be a consequence of the sequence insertion and the lower sequence homology. A detailed examination of the r.m.s. deviations shows that relatively large differences exist in the α2 helix (residues 64–81) of the α/β barrel and a turn-and-coil region (residues 58–63) and also in a fragment (residues 357–364) in the C-terminal domain.

The α2 helices of the α/β barrels in all seven XyIs have r.m.s deviations of 0.2–0.4 Å from each other after superimposition of the C^{α} positions of residues 64–81 (Table 3), indicating that the α2 helices of all seven XyIs have high degree of structural homology. However, the r.m.s deviations between the α2 helices are larger after applying the best superimposition of C^{α} positions 3–63 together with C^{α} positions 82–320 (also shown in Table 3). Therefore, it can be concluded that the α2 helix of the α/β barrel has a different position in different structures. The difference may be caused by the possible flexibility of a turn-and-coil region located at residues 58–63; however, it cannot be determined which specific amino-acid residue might cause the repositioning of the α2 helix (Fig. 1). The helix is far from the active site and is on the surface of the XyI tetramer (Fig. 2*a*); its role in the structure and function of XyI remains to be studied further.

The XyI monomer has a long C-terminal loop which may mediate the interactions between pairs of monomers (Fig. 2). Relatively large differences are observed to occur between fragment 357–364 of SDXyI and those of other *Streptomyces* XyIs. A view of four such fragments superimposed is shown in Fig. 3; the r.m.s. deviations are listed in Table 4, indicating that fragment 357–364 has a higher degree of structural homology in the structures of *Streptomyces* XyIs except, to some extent, SDXyI. By comparing the residue sequences, it seems that the

conformational differences may be caused by the substitution of Pro361 in SDXyI for Val361, which is conserved in other three *Streptomyces* XyIs.

3.3. The metal ions in the active site

The Mg^{2+}, Co^{2+} and Mn^{2+} ions activate the isomerization ability of the xylose isomerase. The enzyme has no activity when dialyzed against a solution containing EDTA for 24 h (Callens *et al.*, 1986; Danno, 1970). Callens *et al.* (1988) reported that the xylose isomerase from *S. violaceoruber* had less than 10% of its maximum activity with one equivalent of Co^{2+} ion per monomer and had over 75% of its maximum activity with two equivalents of Co^{2+} ion per monomer, and that the Co^{2+} ion was superior to Mg^{2+} in protecting the enzyme against thermal denaturation. In the course of the crystallization of SDXyI, the mother liquor contained both Co^{2+} and Mg^{2+} ions. The type of metal ions bound to SDXyI could not be identified previously. The identity of the metal ions in the active site was inferred from the magnitudes of the temperature factors and from the peak heights in the electron-density maps. In the crystal structure previously determined in the pseudo-*I*222 space group (Zhu *et al.*, 1996), two Mg^{2+} ions were assigned per monomer in the positions equivalent to those in other xylose isomerases. However, in the correct space group $P2_12_12$, when two Mg^{2+} ions were placed in each monomer of the present model, all ions had temperature-factor values below 2.0 Å^2 after several cycles of temperature-factor refinement and there was still strong residual electron density at the metal-ion positions. Therefore, the metal ions were reassigned as Co^{2+} ions; there was no remaining electron density in the positions where the metal ions occurred and the temperature factors of the four Co^{2+} ions were all in the range 10–20 Å^2. The SDXyI seemed to prefer to bind Co^{2+} ions rather than Mg^{2+} ions, even though the concentrations of Mg^{2+} and Co^{2+} ions were 0.010 *M* and 0.001 *M*, respectively, in the crystallization solution.

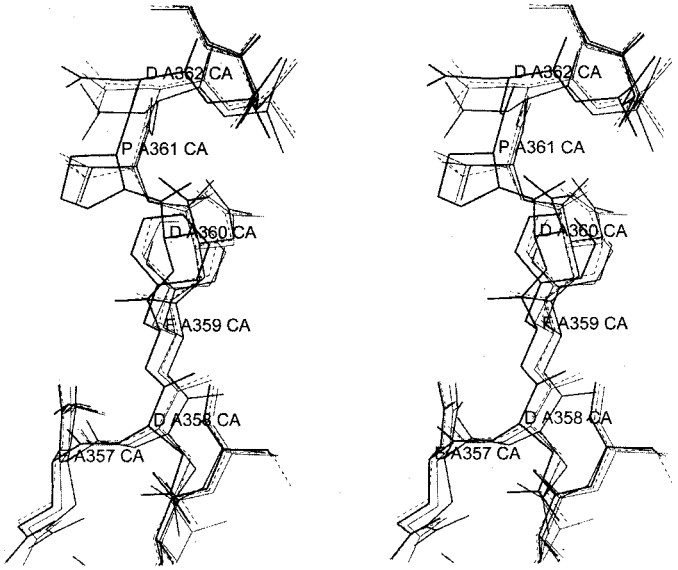

Figure 3
Superimpositions of the fragment Glu357–Ala364 of SDXyI subunit *A* (thick line) and SMXyI (medium line), SRXyI (thin line) and SOXyI (dashed line). The plot was produced using *CHAIN* (Sack, 1988).

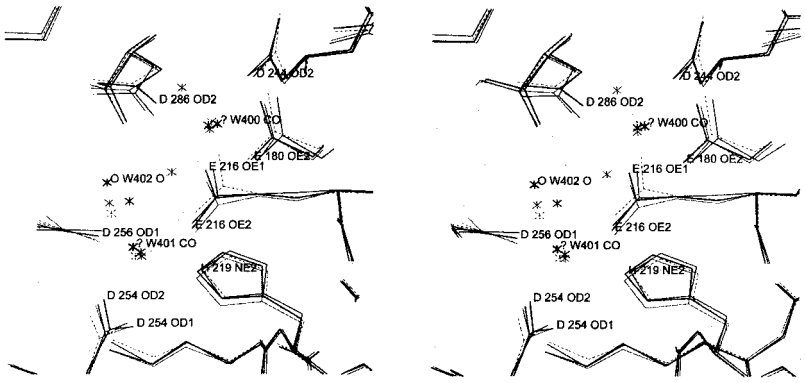

Figure 4
Superimpositions of the metal-binding site of SDXyI subunit *A* (thick line) and ABXyI (medium line), SRXyI (thin line) and SOXyI (dashed line). The plot was produced using *CHAIN* (Sack, 1988).

Table 4
R.m.s. deviations (Å) of C^{α} coordinate positions 357–364 of five structures of *Streptomyces* XyI.

Data are calculated after applying the best superimposition of C^{α} positions 3–320.

	SRXyI	SAXyI	SOXyI	SMXyI
SDXyI	0.670	0.727	0.683	0.847
SRXyI		0.061	0.165	0.338
SAXyI			0.188	0.306
SOXyI				0.431

The active site of SDXyI has two Co^{2+} ions ligated by the side chains of seven amino acids which are conserved in all known xylose isomerases; Table 5 gives the bond lengths and angles between the Co^{2+} ions and their ligands. One metal ion, Co1, has four carboxylate ligands tetrahedrally donated by the carboxylate groups of Glu180, Glu216, Asp244 and Asp286; we do not know what will happen when the substrate binds, as only the native SDXyI structure has been determined. The second metal ion, Co2, has a distorted octahedral coordination and is ligated by three carboxylate groups from Glu216, Asp254 and Asp256, one imidazole of His219 and one water molecule. The distances between the two Co^{2+} ions in subunits *A* and *B* of SDXyI are 4.86 and 4.87 Å, respectively.

The coordinations of the two metal ions reported in the XyI structures are shown in Table 6. A stereoview of the active site in subunit *A* of SDXyI is shown in Fig. 4, which is similar to that of the native AMXyI, SOXyI and ABXyI despite the small twist, but differs from that of the native SRXyI (Whitlow *et al.*, 1991; Carrell *et al.*, 1994) and SMXyI (Rasmussen *et al.*, 1994), in which the metal ions are all hexacoordinated (Table 6). The

Table 5
The bond lengths and angles between the Co^{2+} ions and their SDXyI ligands.

Bond lengths (Å).

Metal	Ligand	Subunit *A*	Subunit *B*	Metal	Ligand	Subunit *A*	Subunit *B*
Co1	Glu180 $O^{\varepsilon 2}$	2.20	2.13	Co2	Glu216 $O^{\varepsilon 2}$	2.25	2.17
	Glu216 $O^{\varepsilon 1}$	1.93	1.99		His219 $N^{\varepsilon 2}$	2.51	2.55
	Asp244 $O^{\delta 2}$	1.90	1.94		Asp254 $O^{\delta 1}$	2.80	2.82
	Asp286 $O^{\delta 2}$	2.06	2.01		Asp254 $O^{\delta 2}$	1.98	2.06
					Asp256 $O^{\delta 1}$	2.17	2.13
					H_2O	2.38	2.20

Angles (°).

	Subunit *A*	Subunit *B*		Subunit *A*	Subunit *B*
Glu180 $O^{\varepsilon 2}$—Co1—Glu216 $O^{\varepsilon 1}$	98.05	96.04	Glu216 $O^{\varepsilon 2}$—Co2—H_2O	104.02	105.70
Glu180 $O^{\varepsilon 2}$—Co1—Asp244 $O^{\delta 2}$	105.30	104.92	His219 $N^{\varepsilon 2}$—Co2—Asp254 $O^{\delta 1}$	85.55	85.71
Glu180 $O^{\varepsilon 2}$—Co1—Asp286 $O^{\delta 2}$	134.93	141.54	His219 $N^{\varepsilon 2}$—Co2—Asp254 $O^{\delta 2}$	88.57	85.33
Glu216 $O^{\varepsilon 1}$—Co1—Asp244 $O^{\delta 2}$	124.55	118.72	His219 $N^{\varepsilon 2}$—Co2—Asp256 $O^{\delta 1}$	150.63	154.21
Glu216 $O^{\varepsilon 1}$—Co1—Asp286 $O^{\delta 2}$	88.91	93.11	His219 $N^{\varepsilon 2}$—Co2—$2H_2O$	112.11	105.96
Asp244 $O^{\delta 2}$—Co1—Asp286 $O^{\delta 2}$	106.85	103.06	Asp254 $O^{\delta 1}$—Co2—Asp254 $O^{\delta 2}$	50.79	49.23
			Asp254 $O^{\delta 1}$—Co2—Asp256 $O^{\delta 1}$	77.10	77.78
Glu216 $O^{\varepsilon 2}$—Co2—His219 $N^{\varepsilon 2}$	69.88	69.86	Asp254 $O^{\delta 1}$—Co2—H_2O	159.85	160.35
Glu216 $O^{\varepsilon 2}$—Co2—Asp254 $O^{\delta 1}$	90.89	93.07	Asp254 $O^{\delta 2}$—Co2—Asp256 $O^{\delta 1}$	98.19	98.27
Glu216 $O^{\varepsilon 2}$—Co2—Asp254 $O^{\delta 2}$	138.12	137.01	Asp254 $O^{\delta 2}$—Co2—H_2O	117.46	114.83
Glu216 $O^{\varepsilon 2}$—Co2—Asp256 $O^{\delta 1}$	86.70	91.18	Asp256 $O^{\delta 1}$—Co2—H_2O	90.11	95.72

coordination difference cannot be explained by the metal ions being co-crystallized or soaked by different metal ions, but may reflect a real difference between XyIs from the different species or may be generated by different distributions of ligated water molecules.

3.4. The water molecules in the structure

There are a total of 636 water molecules in the present SDXyI structure, compared with 396 water molecules in the previous model obtained in the pseudo-*I*222 space group. An approximately equal number of water molecules are associated with each monomer, but there are only 23 pairs of water molecules that occupy equivalent positions in each of the two monomers. Clearly, the positions of water molecules in the previous model have been averaged, which may cause an incorrect distribution of water molecules in the structure. In other words, the correct space group is necessary for the correct identification of the water molecules. For example, water molecule Wat433 in the previous model is ligated to the metal ion of the active site at a distance of 3.70 Å, which is far from the normal value. However, in the present model, the two water molecules are ligated to two metal ions at distances of 2.38 and 2.2 Å. A large proportion of ordered solvent is situated in and around the active-site clefts (Fig. 5), in which the distribution of water molecules is different from that of water molecules in the previous model.

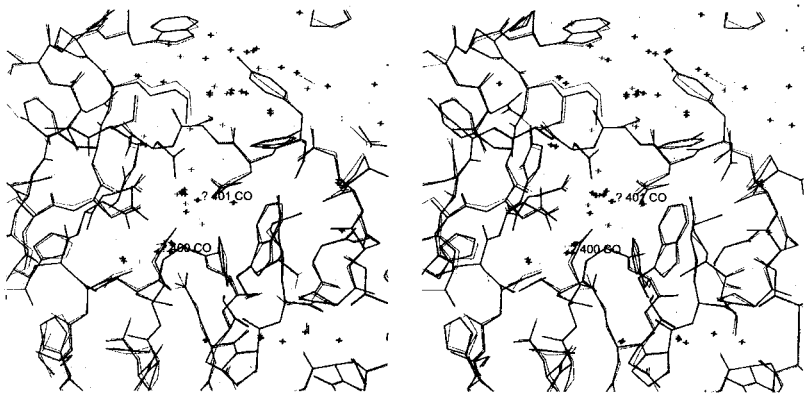

Figure 5
The distribution of water molecules in and around the active-site cleft. The thick lines are the subunit *A* of the refined SDXyI structure; the thin lines are the model previously obtained in the pseudo-*I*222 space group. The plot was produced using *CHAIN* (Sack, 1988).

3.5. The possible dimer in solution

It was found that SDXyI existed as a dimer in solution and that the dimer had catalytic activity (Huang *et al.*, 1992). In principle, the tetramer of SDXyI can be formed by three different combinations of dimers in the crystal (Fig. 2). One of them is the 'butterfly' dimer (made by subunit *A* and subunit *B*; Fig. 2*b*) similar to the 'asymmetric unit' dimer described by Lavie *et al.* (1994). The others are generated by the symmetry operators of space group $P2_12_12$ and are named the 'yin–yang' dimer (made by subunit *A* and an adjacent subunit *A*; Fig. 2*c*) and the 'diagonal' dimer (made by subunit *A* and subunit *B*; Fig. 2*d*), which are also similar to those described by Lavie *et al.* (1994). The problem still remains of which of the three possible dimers is the active dimer in solution. The solvent-accessible surface areas of all three SDXyI dimers were calculated using the program *X-PLOR* with a probe size of 1.6 Å. The interface areas between the two monomers of the 'butterfly', 'yin–yang' and 'diagonal' dimers are 3499, 984 and 3414 $Å^2$, respectively; the values were obtained by adding together the solvent-accessible areas of the two monomers of each dimer and then subtracting the solvent-accessible area of the dimer. Obviously, the 'yin–yang' dimer possesses a monomer-to-monomer interface area three times greater than that of the 'butterfly' or 'diagonal' dimers. It was

Table 6
The average contact distances (Å) between the metal ions and their ligands in the active sites of six XyI structures.

	SDXyI	ABXyI	AMXyI	SOXyI	SRXyI	SMXyI
Metal 1	Co^{2+}	Mn^{2+}	Co^{2+}	Mg^{2+}	Mn^{2+}	Mg^{2+}
Glu180 $O^{\varepsilon1}$	—	—	—	—	—	2.65
Glu180 $O^{\varepsilon2}$	2.17	2.29	2.20	2.40	2.25	2.20
Glu216 $O^{\varepsilon1}$	1.96	2.04	1.95	2.40	2.24	2.10
Asp244 $O^{\delta2}$	1.92	2.24	1.94	2.50	2.22	2.25
Asp286 $O^{\delta2}$	2.04	2.08	2.06	2.40	2.19	2.35
H_2O1	—	—	—	—	2.55	2.40
H_2O2	—	—	—	—	2.66	—
Metal 2	Co^{2+}	Mn^{2+}	Co^{2+}	Mg^{2+}	Mn^{2+}	Mg^{2+}
Glu216 $O^{\varepsilon2}$	2.21	2.22	2.02	2.65	2.16	1.95
His219 $N^{\varepsilon2}$	2.53	2.56	2.39	2.75	2.35	2.90
Asp254 $O^{\delta1}$	2.81	2.50	2.20	2.60	2.31	2.05
Asp254 $O^{\delta2}$	2.02	2.44	2.21	2.55	2.37	2.60
Asp256 $O^{\delta1}$	2.15	2.50	2.11	2.50	2.25	1.90
H_2O	2.29	2.04	2.10	1.90	2.31	1.80

pointed out that xylose isomerase may first aggregate into the 'yin–yang' dimer on an increase in concentration (Lavie *et al.*, 1994). However, the monomers related by the crystallographic twofold axis in the 'yin–yang' dimer come from the same source; the 'yin–yang' dimer may be not a real dimer in solution. The 'butterfly' dimer is the only dimer possessing a intact 'high hydrophobic contrast' in the active site (Lavie *et al.*, 1994). Therefore, further experimental evidence needs to be accumulated in order to determine which dimer of SDXyI is the active dimer in solution.

Financial support for this project was provided by research grants from National 863 Project, National Laboratory of Biomacromolecules and Chinese Academy of Sciences.

References

Allen, K. N., Lavie, A., Petsko, G. A. & Ringe, D. (1995). *Biochemistry*, **34**, 3742–3749.

Amore, R. & Hollenberg, C. P. (1989). *Nucleic Acids Res.* **17**, 7515–7515.

Brünger, A. T. (1992*a*). *X-PLOR, Version* 3.1. *A System for X-ray Crystallography and NMR*. New Haven, Connecticut, USA: Yale University Press.

Brünger, A. T. (1992*b*). *Nature (London)*, **355**, 472–475.

Callens, M., Kersters-Hilderson, H., Vangrysperre, W. & De Bruyne, C. K. (1988). *Enzyme Microb. Technol.* **10**, 695–700.

Callens, M., Kersters-Hilderson, H., Van Opetal, O. & De Bruyne, C. K. (1986). *Enzyme Microb. Technol.* **8**, 696–700.

Carrell, H. L., Glusker, J. P., Burger, V., Manfre, F., Tritsch, D. & Biellmann, J.-F. (1989). *Proc. Natl Acad. Sci. USA*, **86**, 4440–4444.

Carrell, H. L., Hoier, H. & Glusker, J. P. (1994). *Acta Cryst.* D**50**, 113–123.

Carrell, H. L., Rubin, B. H., Hurley, T. J. & Glusker, J. P. (1984). *J. Biol. Chem.* **259**, 3230–3236.

Collyer, C. A., Henrick, K. & Blow, D. M. (1990). *J. Mol. Biol.* **212**, 211–235.

Danno, G. (1970). *Agric. Biol. Chem.* **34**, 1805–1814.

Danno, G. (1971). *Agric. Biol. Chem.* **35**, 997–1006.

Dauter, Z., Terry, H., Witzel, H. & Wilson, K. S. (1990). *Acta Cryst.* B**46**, 833–841.

Farber, G. K., Petsko, G. A. & Ringe, D. (1987). *Protein Eng.* **1**, 459–466.

Hendrickson, W. A. & Konnert, J. (1981). *Biomolecular Structure, Function, Conformation and Evolution*, edited by R. Srinivasan, Vol. 1, pp. 43–47. Oxford: Pergamon Press.

Henrick, K., Blow, D. M., Carrell, H. L. & Glusker, J. P. (1987). *Protein Eng.* **1**, 467–469.

Henrick, K., Collyer, C. A. & Blow, D. M. (1989). *J. Mol. Biol.* **208**, 129–157.

Howard, A. J., Gilliland, G. L., Finzel, B. C., Poulos, T. L., Ohlendorf, D. H. & Salemme, F. R. (1987). *J. Appl. Cryst.* **20**, 383–387.

Huang, W., Wang, C., Liu, J., Cui, T., Liu, X., Niu, L., Wang, Y. & Xu, X. (1992). *J. China Univ. Sci. Technol.* **22**(3), 283–289.

Jenkins, J., Janin, J., Rey, F., Chiadmi, M., Van Tilbeurgh, H., Lasters, I., De Maeyer, M., Van Belle, D., Wodak, S. J., Lauwereys, M., Stanssens, P., Mrabet, N. T., Snauwaert, J., Matthyssens, G. & Lambeir, A.-M. (1992). *Biochemistry*, **31**, 5449–5458.

Jones, T. A., Zou, J.-Y., Cowan, S. W. & Kjeldgaard, M. (1991). *Acta Cryst.* A**47**, 110–119.

Kraulis, P. J. (1991). *J. Appl. Cryst.* **24**, 946–950.

Lambeir, A.-M., Lauwereys, M., Stanssens, P., Mrabet, N. T., Snauwaert, J., Van Tilbeurgh, H., Matthyssens, G., Lasters, I., De Maeyer, M., Wodak, S. J., Jenkins, J., Chiadmi, M. & Janin, J. (1992). *Biochemistry*, **31**, 5459–5466.

Lavie, A., Allen, K. N., Petsko, G. A. & Ringe, D. (1994). *Biochemistry*, **33**, 5459–5480.

Loviny-Anderton, T., Shaw, P. C., Shin, M. K. & Hartley, B. S. (1991). *Biochem. J.* **277**, 263–271.

Luzzati, P. V. (1952). *Acta Cryst.* **5**, 802–810.

Rasmussen, H., La Cour, T., Nyborg, J. & Schülein, M. (1994). *Acta Cryst.* D**50**, 124–131.

Rey, F., Jenkins, J., Janin, J., Lasters, I., Alard, P., Claessens, M., Matthyssens, G. & Wodak, S. (1988). *Proteins Struct. Funct. Genet.* **4**, 165–172.

Rose, I. A., O'Connell, E. L. & Mortlock, R. P. (1969). *Biochim. Biophys. Acta*, **178**, 376–379.

Sack, J. S. (1988). *J. Mol. Graph.* **6**, 224–225.

Van Tilbeurgh, H., Jenkins, J., Chiadmi, M., Janin, J., Wodak, S. J., Mrabet, N. T. & Lambeir, A.-M. (1992). *Biochemistry*, **31**, 5467–5471.

Wang, Y., Huang, Z., Dai, X., Liu, J., Cui, T., Niu, L., Wang, C. & Xu, X. (1994). *Chin. J. Biotechnol.* **10**, 97–103.

Whitlow, M., Howard, A. J., Finzel, B. C., Poulos, T. L., Winborne, E. & Gilliland, G. L. (1991). *Proteins Struct. Funct. Genet.* **9**, 153–173.

Wong, H. C., Ting, Y., Lin, H. C., Reichert, F., Myambo, K., Watt, K. W., Toy, P. L. & Drummond, R. J. (1991). *J. Bacteriol.* **173**, 6849–6858.

Zhang, G. Y., Niu, L. W., Huang, W. Z., Wang, C., Liu, J., Cui, T., Liu, X. A., Wang, Y. Z., Xu, X. & Liang, D. C. (1991). *Chin. Sci. Bull.* **36**, 1646–1649.

Zhu, X., Gong, W., Niu, L., Teng, M., Xu, Q., Wu, C., Cui, T., Wang, Y. & Wang, C. (1996). *Sci. China (Ser. C)*, **39**, 636–644.